# Building Energy Doctors: An SPC and Kalman Filter-Based Method for System-Level Fault Detection in HVAC Systems

Biao Sun, *Student Member, IEEE*, Peter B. Luh, *Fellow, IEEE*, Qing-Shan Jia, *Senior Member, IEEE*, Zheng O'Neill, and Fangting Song

***Abstract*—Buildings worldwide account for nearly 40% of global energy consumption. The biggest energy consumer in buildings is the Heating, Ventilation and Air Conditioning (HVAC) systems. HVAC also ranks top in terms of number of complaints by tenants. Maintaining HVAC systems in good conditions through early fault detection is thus a critical problem. The problem, however, is difficult since HVAC systems are large in scale, consisting of many coupling subsystems, building and equipment dependent, and working under time-varying conditions. In this paper, a model-based and data-driven method is presented for robust system-level fault detection with potential for large-scale implementation. It is a synergistic integration of: ) Statistical Process Control (SPC) for measuring and analyzing variations; 2) Kalman filtering based on gray-box models to provide predictions and to determine SPC control limits; and (3) system analysis for analyzing propagation of faults' effects across subsystems. In the method, two new SPC rules are developed for detecting sudden and gradual faults. The method has been tested against a simulation model of the HVAC system for a 420-meter-high building. It detects both sudden faults and gradual degradation, and both device and sensor faults. Furthermore, the method is simple and generic, and has potential replicability and scalability.**

***Note to Practitioners*—HVAC systems work under time-varying weather and cooling load, and it is therefore difficult to detect faults. In addition, the various devices of HVAC systems require the detection method simple and robust so that it has good replicability and scalability. A gray-box model-based and data-driven method is developed in this paper. It is a novel combination of SPC, Kalman filter, and system analysis. By measuring and analyzing variations of model parameters, a fault can be detected when it causes these parameters to deviate from their normal ranges. The method detects both sudden and gradual faults with high detection rate and low false alarm rate. It also detects effects of faults in one subsystem on another to help detect and confirm device faults.**

***Index Terms*—Fault detection, heating, ventilation and air conditioning (HVAC), Kalman filter, statistical process control (SPC).**

Manuscript received September 15, 2012; accepted October 13, 2012. This paper was recommended for publication by Associate Editor J. Li and Editor M. C. Zhou upon evaluation of the reviewers' comments. This paper was presented in part at the IEEE Conference on Automation Science and Engineering, Trieste, Italy, August 2011.

B. Sun and Q.-S. Jia are with the Center for Intelligent and Networked Systems (CFINS), Department of Automation, Tsinghua University, Beijing 100084, China (e-mail: sun-b05@mails.tsinghua.edu.cn; jiaqs@tsinghua.edu.cn).

P. B. Luh is with the Department of Electrical and Computer Engineering, University of Connecticut, Storrs, CT 06269-2157 USA (e-mail: Peter.Luh@uconn.edu).

Z. O'Neill is with the United Technology Research Center, Hartford, CT 06118 USA (e-mail: oneillz@utrc.utc.com).

F. Song is with the United Technology Research Center, Shanghai 201204, China (e-mail: SongFT@utrc.utc.com).

Color versions of one or more of the figures in this paper are available online at http://ieeexplore.ieee.org.

Digital Object Identifier 10.1109/TASE.2012.2226155

## I. Introduction

BUILDINGS worldwide account for nearly 40% of global energy consumption and a significant share of greenhouse gas emissions [2]. The biggest energy consumer in buildings is the Heating, Ventilation, and Air Conditioning (HVAC) systems. HVAC also ranks top in terms of number of complaints by building tenants. Maintaining HVAC systems in good conditions is thus a critical issue. Although regular maintenance can and should be scheduled, it may not be able to detect faults soon enough. Improving performance of HVACs through early fault detection and reducing the maintenance cost are thus of great value.

A typical HVAC system is depicted in Fig. 1. It consists of multiple interconnected subsystems—Air Handling Units (AHUs), chillers, cooling towers, pumps, ducts, etc. A subsystem (e.g., chiller subsystem) may consist of multiple devices (e.g., chillers). Consider a summer day as an example. Indoor air temperature is decreased by supplying cool air from an AHU to rooms. In an AHU, hot air returning from rooms together with hot fresh air is cooled by chilled water supplied from chillers. After having heat exchange with the air in the AHU, the chilled water with its temperature increased then returns to chillers. Chillers are used to decrease the return chilled water temperature by transferring its extra heat to cooling water which is supplied from cooling towers. After the cooling water returns to cooling towers, the extra heat it contains is transferred to outside air by using cooling tower fans.

Fault detection in HVAC systems is difficult because the systems are generally large in scale with complicated couplings among subsystems through water and air flows, building and equipment dependent, and working under time-varying weather and cooling load. As presented in Section II, most fault detection methods in the literature are at the device level but not at the system level where propagation of faults' effects across subsystems is considered; and many methods require focused studies on individual buildings for a long period of time with poor replicability and scalability.

In this paper, a simple and robust fault detection method is developed to detect both sudden faults and gradual degradation of devices and their associated sensors while considering

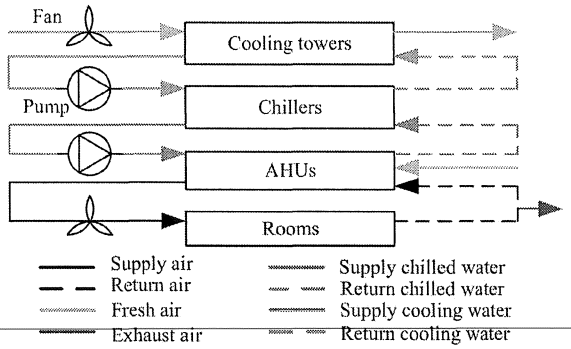


Fig. 1. A typical HVAC system consisting of AHUs, chillers, cooling towers, etc.

propagation of faults' effects across subsystems. The method is model-based and data-driven. In Section III, "gray-box" models of a chiller and a cooling tower taken from the literature are presented, where the characteristics of each of the above devices are summarized by a few key parameters. Different from "black-box" models that only use measured data to represent key characteristics of a device, gray-box models use physical knowledge together with measured data, and are more robust than black-box models for fault detection.

In Section IV, a novel fault detection method is presented. In the method, Statistical Process Control (SPC) is used for measuring and analyzing gray-box model parameters' variations caused by faults. The standard SPC with static control limits, however, results in many false alarms because the time-varying weather and cooling load can also cause the parameters to deviate from their normal ranges. To overcome this difficulty, Kalman filtering based on gray-box models is used to determine adaptive SPC control limits. In a Kalman filter, the states are gray-box model parameters. The states and their covariance are estimated based on data from sensors. The adaptive SPC control limits are a few standard deviations, which are obtained from the covariance of states, around the average of states estimated over a past time period. In traditional SPC rules without Kalman filtering, back-to-back estimates of a parameter are usually independent, and therefore the SPC rule using back-to-back estimates outside SPC control limits can be easily developed to satisfy given false alarm rate and detection rate [3]. However, when SPC is combined with Kalman filtering, back-to-back estimates are not independent. Therefore, based on the adaptive SPC control limits, two new SPC rules which consider the dependence caused by Kalman filtering are developed for detecting sudden and gradual faults.

As presented in Section V, a fault in one HVAC subsystem may affect another subsystem in terms of water or air temperature, energy consumption, etc., through the coupling of water or air flows between them. A systematic analysis of the propagation of fault effects can help detect and confirm a device fault. In view that the gray-box models used for detecting device faults describe device characteristics rather than flow balance or energy conservation, such system-wide analysis is not straightforward. Our idea is to introduce "coupling variables" between subsystems to capture their interactions. SPC is then performed on the differences between measured and predicted coupling variables. This is done without the need to create a big Kalman filter for the aggregate model of coupled subsystems. There is no major increase in complexity as compared to the device-level fault detection except the addition of coupling variables and the associated SPC rules. Our method thus has good scalability and can detect and confirm a device fault.

In Section VI, a simulation model of the HVAC system in the Jinmao Tower, a famous building in Shanghai with 88 floors, is used to test our fault detection method. This model is also used in Section IV to help illustrate the method developed. The testing results show that the method detects sudden faults, gradual faults, and propagation of faults' effects across subsystems. Complete testing data and results for two simple cases are provided for duplicating the fault detection.

Our preliminary results on the method were presented in [1]. In [4], we also extended the method for an air-cooled chiller, which was cooled by air rather than by cooling water from cooling towers, as shown in Fig. 1. Based on [1] and [4], the method is further improved with rigorous derivations to obtain SPC rules which have high detection rate and low false alarm rate. The detection of successive faults and the further study on propagation of faults' effects across subsystems are included. Numerical testing is strengthened with a more detailed description of the complicated HVAC system in the Jinmao Tower. Also, the entire paper has been improved with more insights provided.

## II. Literature Review

Most fault detection methods in the literature are at the device level, such as chillers, cooling towers, and AHUs ([5]–[16]), but not at the system level where the effects of faults in one subsystem on another are considered. For device-level fault detection, most methods are based on models, either detailed physical models, or black-box models, or gray-box ones. The general idea of model-based fault detection is to describe a device using correlations among input and output variables, and evaluate their changes such as residuals between measured variables and the ones predicted by models.

In physical HVAC models [5], [6], a set of detailed mathematical equations based on mass and energy balances are established to capture the characteristics of HVACs. For fault detection, these models are used to predict the outputs with inputs obtained from sensors. The model outputs are then compared with the corresponding sensor measurements to generate residuals. A fault is detected if the absolute values of residuals are higher than given thresholds. In [5], a physical chiller model was established to predict several chiller characteristic quantities (CQs), e.g., chiller COP, for fault detection purpose. Simulation results showed that faults were detected when measured characteristic quantities under faults deviated from their normal values predicted by models. Physical models, however, require many inputs to describe a device and some may not be available in buildings. Also, the physical models can be complex, leading to high computational requirements [17]. Therefore, fault detection methods based on physical models have a limited scalability. In addition, if the given threshold is improper, the absolute values of residuals might be lower than the threshold even though there is a fault. The fault will not be detected because of the improper threshold. One way to detect the fault is to decrease the threshold but this will also result in a higher false

alarm rate. Therefore, thresholds of deviations were not easy to determine for fault detection, especially when measurement noises and model inaccuracy were considered.

For black-box models, relationships between inputs and outputs are described by using model parameters that have no physical meanings. Various methods can be used to establish black-box models, including regression [7], [8], principal component analysis [9]–[11], artificial neural networks [12], pattern recognition [13], and multiple-model adaptive estimation algorithm [14], [15]. For example, in [7], a black-box polynomial model, with its parameters obtained based on training data, was used to predict temperatures in a chiller under normal conditions. Differences between these predicted temperatures and measured ones were used as indicators for faults.

Unlike conventional black-box models using parameters to describe correlations between inputs and outputs, a PCA method considers correlations buried in data and uses pure mathematical data-driven models to derive statistics. The statistics are then used to validate the correlations to detect faults. For example, in [9], a PCA-based method used the Q statistic (i.e., squared prediction error) to detect AHU sensor faults and the Q contribution plots supplemented by expert rules to diagnose faults.

Black-box models are easy to established and often require less computational capacity than physical models [17]. A large amount of training data and a long time for focus study, however, are needed to train black-box models. Furthermore, fault detection methods based on black-box models have limited robustness because the data beyond the range of training data might result in false alarms. In addition, their abilities in fault isolation may be restricted in view that black-box models generally do not have clear physical meanings.

Unlike black-box models using only measured inputs and outputs to represent characteristics of a device, gray-box models use physical knowledge about a device in combination with measured data [16]. Since parameters predicted by gray-box models tend to be more robust than those by black-box models, gray-box models have better potential for robust fault detection, and can also provide insights and understanding of faults [17] for fault diagnosis.

In [16], a gray-box chiller model with a few parameters was used for fault detection. By using linear regressions, the averages of the parameters and their standard deviations were obtained from data without any faults. If faults occurred, the regressed parameters deviated from their averages. Faults were detected when the deviation was larger than one or two standard deviations. The method was tested based on published data from a centrifugal chiller. The method, however, was not verified with time-varying weather and cooling load. It therefore did not consider the false alarm problem (presented in details in Section IV-A) that might be caused by the time-varying weather and cooling load.

SPC has been widely used for fault detection in many fields, e.g., manufacturing system [18] and medical treatment [19]. The key idea of the SPC is first to select parameters which can be considered as constants to reflect characteristics of a system. These parameters would only have natural variation caused by measurement noises and process noises under normal conditions. If there was any fault, they should deviate from their normal ranges and the fault should be picked up by SPC control limits. However, no major applications to HVAC systems have been reported. This might be caused by the fact that HVAC systems are operated under time-varying weather and cooling load and it is difficult to determine SPC control limits which have high detection rate but low false alarm rate.

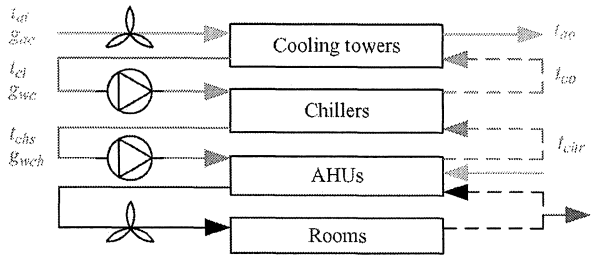


Fig. 2. Temperatures and flow rates needed for the HVAC models.

## III. Gray-Box Models

Gray-box models for chillers and cooling towers are selected from the literature and presented in Sections III-A and III-B, respectively. These models describe performances of devices working under a range of conditions.

### A. A Gray-Box Model for Chillers

The gray-box model selected for chillers is a simple and universal model developed by Gordon and Ng [20]. It has been proved to be accurate for a large number of chiller types and sizes [21]. It is not an energy balance or mass balance equation. Rather, the parameters capturing key characteristics of a chiller are considered as the state variables. Variables such as temperatures and water flow rates are obtained from sensor measurements and used to estimate the model parameters.

The model is given by

$$\left(\frac{1}{\mathrm{COP}}+1\right)\frac{t_{chr}}{t_{ci}}-1=a_1\frac{t_{chr}}{L_{ch}}+a_2\frac{t_{ci}-t_{chr}}{t_{ci}L_{ch}}+a_3\left(\frac{1}{\mathrm{COP}}+1\right)\frac{L_{ch}}{t_{ci}} \quad (1)$$

where $a_1$, $a_2$, and $a_3$ are three model parameters or state variables, with $a_1$ being the chiller internal entropy production rate, $a_2$ the heat losses (or gains) rate from (or into) the chiller, and $a_3$ the heat exchange thermal resistance and related to the evaporator and condenser. As shown in Fig. 2, $t_{chr}$ in (1) is return chilled water temperature from AHUs to the chiller, and $t_{ci}$ the inlet water temperature from cooling towers to the chiller. The Coefficient of Performance (COP), representing how many units of cooling amount are generated by each unit of electricity, is an indicator of the chiller's energy efficiency. It is calculated as the ratio of chiller cooling load $L_{ch}$ divided by chiller electrical power $P_{ch}$. The chiller cooling load $L_{ch}$ equals energy difference between return chilled water and supply chilled water as

$$L_{ch}=C_w g_{wch}(t_{chr}-t_{chs}) \quad (2)$$

where $C_w$ is the water heat capacity, $g_{wch}$ chilled water flow rate, and $t_{chs}$ supply chilled water temperature. All variables except the three parameters in the models should be measurable

or calculable from measured data. In (1) and (2), $t_{chr}$, $t_{ci}$, $t_{chs}$ and $g_{wch}$ are measured variable and used as inputs to the model.

In the literature [20], the parameters of the gray-box chiller model are obtained from historical data using least square method and are constant. The model is often used to calculate the output chiller power, given the input water temperatures and cooling load.

### B. A Gray-Box Model for Cooling Towers

The cooling tower model developed by Lichtensien [22] is selected for our use. It uses three model parameters $b$, $m$, and $n$ to capture key characteristics of a cooling tower as

$$\beta_d F_c = b g_{wc}^m g_{ac}^n \tag{3}$$

where $g_{wc}$ is cooling water flow rate, $g_{ac}$ the air flow rate, $\beta_d$ the mass conductivity coefficient of the cooling water, and $F_c$ the cooling tower heat exchange area. In the above, $b$ and $m$ reflect the effect of cooling water flow rate on $\beta_d$, and $b$ and $n$ reflecting the effect of air flow rate on $\beta_d$. The term $\beta_d F_c$ is calculated using the heat exchanger model in [23] as

$$\beta_d F_c = q_{ct}/\Delta i \tag{4}$$

where $q_{ct}$ is the heat exchanged between cooling water and outside air, and $\Delta i$ the logarithmic-mean difference between saturated air enthalpy $i_{\text{sat}}$ at the water air-water interface and outside air enthalpy $i_{\text{out}}$.

The outside air enthalpy $i_{\text{out}}$ can be calculated based on measured temperature and humidity. If no sensor is available for humidity, it can also be calculated by using an empirical formula based only on wet bulb temperature $t_{wb,\text{out}}$ as

$$i_{\text{out}} = p_0 + p_1 t_{wb,\text{out}} + p_2 t_{wb,\text{out}}^2 + p_3 t_{wb,\text{out}}^3. \tag{5}$$

In the above, $p_0, p_1, p_2$, and $p_3$ are parameters obtained by using a fitting technique.

The water flow rate $g_{wc}$ can be measured by a sensor. If there is only one sensor available to measure the mixed cooling water flow rate from all cooling towers, then the water flow rate for each cooling tower can be calculated from the measured mixed flow rate using water pressure balance and water flow balance. The detailed calculation is presented in Section VI-A by using the HVAC system in Jinmao Tower as a case study. Since air flow rate $g_{ac}$ can be approximately regarded as a function only of its fan frequency, it can be obtained based on fan frequency and a lookup table. Similar to the gray-box chiller model, this cooling tower model is often used to calculate the outlet cooling water temperature given all the inputs and parameters, which are obtained from data and constant.

## IV. SPC and Kalman Filter-Based Fault Detection Method

In this section, the SPC and Kalman filter-based method for HVAC fault detection is developed. The key idea of the method to detect device and sensor faults is presented in Section IV-A. The Kalman filtering using gray-box models to provide predictions and determine SPC control limits is presented in Section IV-B. The SPC rule for detecting sudden faults is developed in Section IV-C, and the SPC rule for gradual faults is developed in Section IV-D. Some discussions are then presented in Section IV-E.

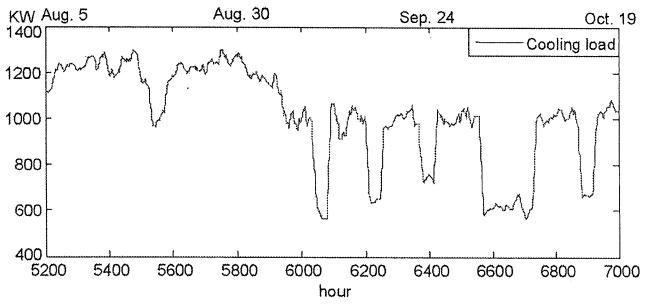


Fig. 3. The cooling load of the chiller.

### A. The Key Idea of SPC and Kalman Filter-Based Fault Detection Method

To detect a device fault, our idea of SPC and Kalman filter-based method is to view model parameters of the device as a slowly changing state $x$, driven by time-varying weather, cooling load, etc. If there is no fault, then ideally the state should be within a normal range, i.e., SPC control limits; if there is a device fault, then the state may deviate from its normal range and the fault can be picked up by an SPC rule. For a fault of a sensor associated with the device, although nothing is wrong with the device, the faulty values from the sensor will cause the Kalman filter to give a faulty estimation of the state. Therefore, the estimated state will also deviate from its normal range and the sensor fault will be detected.

Static SPC control limits can be derived from manufacturer specifications or from "good data" when the device is operated in good conditions. Although the traditional use of the gray-box models is to give constant model parameters, e.g., state, to calculate the model outputs as presented in the last section, the state changes under the influences of cooling load (as presented in Fig. 3) as a result of time-varying weather, schedule, etc. In addition, the simplicity of the model might also cause the state to change with time. Therefore, many false alarms may arise under the static control limits because of the changing of state. For illustration, the estimated parameter $a_1$ for a chiller under a no-fault condition for the Shanghai Jinmao Tower is shown in Fig. 4. The parameter's normal range, i.e., static SPC control limits, is plus and minus two-sigma's, which are obtained from means and standard deviations of good data for $a_1$. By comparing the cooling load for the chiller in Fig. 3 and the parameter $a_1$ in Fig. 4, it can be seen that $a_1$ shifts slowly as the cooling load changes, and lies outside the static SPC control limits many times even when there is no fault, resulting many false alarms if such a static control limit is used.

To overcome the above false alarm difficulty, Kalman filtering is used to obtain adaptive SPC control limits. Although Kalman filtering is traditionally used to estimate the state and output of a dynamic system, it can also be used to estimate the slowly-varying parameters (treated as the state) of a gray-box model. The state and its covariance matrix can then be derived

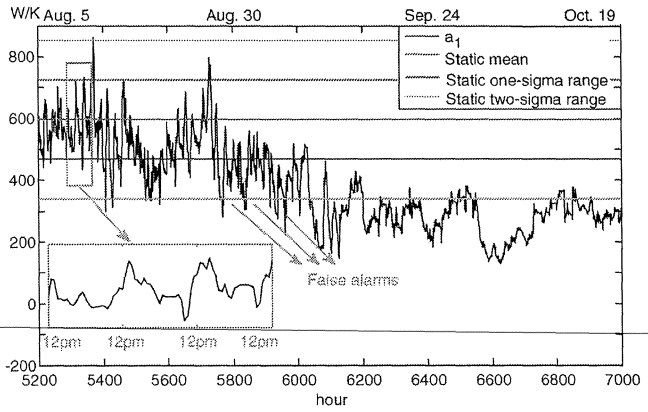


Fig. 4. The parameter $a_1$ and the static SPC control limits under normal condition.

based on the standard Kalman filtering equations and data from sensors. The adaptive SPC control limits can then be derived, e.g., two standard deviations around the average of the state estimated over past 24 h, as will be derived in Section IV-C.

### *B. Kalman Filtering Based on Gray-Box Models to Provide Predictions and Determine SPC Control Limits*

The abstract gray-box models of chiller and cooling towers in Section III are static, but their parameters used to capture thermal characteristics of devices vary slowly rather than remain constant over time. We are not looking at the dynamics of a device or trying to develop a dynamic diagnosis method. Rather, the Kalman filter is used to estimate the model parameters based on the gray-box models and data measured by sensors for fault detection.

*State Equation and Output Equation:* Consider first the chiller model (1). The model parameters $a_1$, $a_2$, and $a_3$ are three elements of the state $x$. These parameters change slowly over time as might be caused by time-varying cooling load, the simplicity of the model, etc. Process noises are introduced to account for the variations. If the standard Kalman filter formulation is to be used, the process noise $w_k$ is usually assumed to be zero-mean

$$x_{k+1} = x_k + w_k \tag{6}$$

where the time interval is assumed to one hour for convenience of presentation.

As shown in Fig. 4, $w_k$, however, varies in a day-and-night pattern as the cooling load varies and therefore is not zero-mean. To avoid this cause of not being zero-mean, the process noise is redefined to explicitly consider such daily variations as follows:

$$w_k = (x_{k+1} - x_k) - (\hat{x}_{k-23} - \hat{x}_{k-24}) \tag{7}$$

where $\hat{x}_{k-23}$ and $\hat{x}_{k-24}$ are the given state estimates at time $k-23$ and time $k-24$, respectively. This noise $w_k$ is assumed to be zero mean.

Based on (7), the state (6) is modified to

$$x_{k+1} = x_k + (\hat{x}_{k-23} - \hat{x}_{k-24}) + w_k. \tag{8}$$

To obtain the output equation, the left-hand side of (1) is viewed as the measurement $z$. It is calculated based on $t_{chr}$, $t_{chs}$, $t_{ci}$, and $g_{wch}$ (see (1) and (2)) which are obtained from sensor measurements. From (1), it is clear that $z_k$ at time $k$ is a linear function of $x_k$ as

$$z_k = H_k x_k + v_k \tag{9}$$

where

$$H_k = \left[\frac{t_{chr,k}}{L_{ch,k}}, \frac{t_{ci,k} - t_{chr,k}}{t_{ci,k} L_{ch,k}}, \frac{(1/\mathrm{COP}_k + 1) L_{ch,k}}{t_{ci,k}}\right]$$

and $v_k$ is the measurement noise. With the above linear state and output equations, standard Kalman filter formulations can be used [to be presented in (11) and (12)].

*Process and Measurement Noise Covariance Matrices:* It is assumed that the random variables $w_k$ and $v_k$ are independent. For simplification, process noises are assumed white, zero mean, and Gaussian with process covariance matrix $Q_k$. In addition, based on product manuals of sensors, measurement noises are also assumed white, zero-mean, and Gaussian with measurement noise covariance matrix $R_k$. The matrices $Q_k$ and $R_k$ affect the convergence and accuracy of the state estimated in a Kalman filter, but they are usually difficult to be obtained accurately.

Since process noises in (8) are affected by time-varying weather and cooling load, the process noise covariance matrix $Q$ changes with time and therefore is estimated based on historical process noises as presented next.

The process noise at time $k$ is estimated according to (7) as

$$w_k = (\hat{x}_{k+1} - \hat{x}_k) - (\hat{x}_{k-23} - \hat{x}_{k-24}) \tag{10}$$

where $\hat{x}$ is the estimated state [explained after (11)]. The process noise covariance matrix $Q_k$ at time $k$ is calculated as the covariance matrix of the estimated process noises in the past $m$ hours (from hour $k-m$ to hour $k-1$).

Upon initialization before the $m$ estimated process noises (10) become available, $Q_k$ is estimated based on experience. One way to select an appropriate value of $m$ follows the steps below.

Step 1) Initialize $m$ to 24.

Step 2) Use the Kalman filter to estimate the state [presented later in (11), (12)], estimate process noises in (10) and estimate $Q_{k'}$ ($k'$ is given and much larger than $m$) based on process noises.

Step 3) Increase $m$ by 24 since process noises have a pattern of 24 h as the cooling load does.

Step 4) Repeat Steps 2 and 3 until the changing of matrix 2-norm of $Q_{k'}$ is less than a given small threshold.

The measurement $z$ in (9) is calculated based on measured variables $t_{chr}$, $t_{chs}$, $t_{ci}$, and $g_{wch}$. The sensor noises of the four variables depend on their measured values, e.g., the sensor noise for $g_{wch}$ is $\pm 1\%$ of the measured flow rate with a confidence level of 95%. The measurement noise covariance matrix $R$ therefore changes with measurements. At time $k$, $R_k$ is estimated by using Monte Carlo simulation based on measured

values of $t_{chr,k}$, $t_{ci,k}$, $t_{chs,k}$, and $g_{wch,k}$, and their sensor noises as follows

Step 1) Obtain measured values of $t_{chr,k}$, $t_{ci,k}$, $t_{chs,k}$, and $g_{wch,k}$ from sensors in a building; generate $m$ (e.g., 1000) sets of noises for the fours variables based on their sensor noise distributions obtained from manufacturer specifications; generate $m$ sets of values of the four variables by adding $m$ sets of noises to their measured values.

Step 2) Calculate $m$ measurements $z_{k,1}, \ldots, z_{k,m}$ according to the left-hand side of (1) by using the $m$ sets of values of the four variables in Step 1.

Step 3) Calculate $R_k$ as the variance of $z_{k,1}, \ldots, z_{k,m}$.

*Kalman Filter for Models of Chillers:* The Kalman filter consists of two steps: time update and measurement update. In the time update, the state is projected ahead as [24], [25]

$$\hat{x}_{k+1}^{-} = \hat{x}_k \tag{11}$$

where $\hat{x}_{k+1}^{-}$ is the priori state estimation at time $k+1$ given knowledge of the process prior to time $k+1$; and $\hat{x}_k$ is the posteriori state estimate at time $k$ given measurement $z_k$.

In the measurement update with measurement equals $z_{k+1}$, the state estimation is then updated to $\hat{x}_{k+1}$

$$\hat{x}_{k+1} = \hat{x}_{k+1}^{-} + K_{k+1}\left(z_{k+1} - H_{k+1}\hat{x}_{k+1}^{-}\right) \tag{12}$$

where $K_{k+1}$ is the Kalman gain. It is calculated based on $Q_{k+1}, R_{k+1}$, and the state covariance matrix $P_k$ which can also be estimated in the Kalman filter [24], [25]. The roots of diagonal elements of $P_k$ are the standard deviations of model parameters.

By substituting (11) to (12), the state at time $k$ can be estimated from the previous estimate and the current measurement, i.e.,

$$\hat{x}_{k+1} = \hat{x}_k + K_{k+1}(z_{k+1} - H_{k+1}\hat{x}_k). \tag{13}$$

*Adaptive SPC Control Limits:* To detect faults and reduce false alarms in Fig. 4, adaptive SPC control limits rather than static ones are used. The averages of parameters estimated over the past $K$ hours are used as normal values of the state. The two-sigma range around normal values is defined as the adaptive SPC control limits in the rest of this paper. The two-sigma range, using $a_1$ of a chiller model at time $k$ as an example, is defined as

$$[\overline{\mu}_{1,k} - 2\overline{\sigma}_{1,k}, \overline{\mu}_{1,k} + 2\overline{\sigma}_{1,k}] \tag{14}$$

where $\overline{\mu}_{1,k}$ is the mean of $\hat{a}_1$ estimated over the past $K$ hours as

$$\overline{\mu}_{1,k} = \frac{1}{K}\sum_{i=k-K+1}^{k} \hat{a}_{1,i} \tag{15}$$

and $\overline{\sigma}_{1,k}$, the averaged standard deviation at time $k$, is averaged in the same way. The one-sigma range is similarly defined. With the above adaptive SPC control limits, SPC rules for detecting sudden and gradual faults are then developed in the next two subsections. The value of $K$ is also determined in the development of SPC rules.

### C. SPC Rule for Detecting Sudden Faults

Consider a sudden fault first in this subsection and a gradual fault in the next subsection. To detect a sudden fault, the SPC rule we selected is that a fault is detected if $n$ back-to-back estimates of a parameter (e.g., $\hat{a}_{1,k-n+1}, \hat{a}_{1,k-n+2}, \ldots, \hat{a}_{1,k}$) fall outside its adaptive two-sigma range defined in (14). As $n$ increases, a fault will be detected with increasing confidence and therefore the false alarm rate will decrease. A large $n$, however, will result in a low detection rate, since a fault which causes a parameter lying outside two-sigma range in less than $n$ successive hours will not be detected. To keep a balance between the false alarm rate and the detection rate, our idea is to set $n$ as low as possible to increase detection rate but large enough to maintain a false alarm rate below 1%.

In traditional SPC rules without Kalman filtering, $n$ back-to-back estimates are independent, and it is easy to calculate the false alarm rate given $n$ and the distributions of the estimates. However, when the SPC is combined with Kalman filtering, the $n$ back-to-back estimates are not independent because the estimate $\hat{x}_{k+1}$ at time $k+1$ is affected by the previous estimate $\hat{x}_k$ at time $k$, as shown in (13). Therefore, in the rest of this section, the value of $n$ is first determined, considering the dependence of $n$ back-to-back estimates. Then, the value of $K$ is determined to obtain the adaptive SPC control limits, and the SPC rule with adaptive control limits is used to detect a sudden fault for illustration. In addition, the reason of using two-sigma rather than one- or three-sigma range is presented at the end of this subsection because the explanation requires the determination of $n$.

*Determining n Based on False Alarm Rate:* To find the minimal $n$ to maintain a false alarm rate below 1%, the relationship between $n$ and the false alarm rate is needed. Consider $\hat{a}_1$ of a chiller model as an example. The false alarm rate at time $k$ equals the probability of $n$ successive estimates $\hat{a}_{1,k-n+1}, \hat{a}_{1,k-n+2}, \ldots, \hat{a}_{1,k}$ lying outside the two-sigma range when the chiller works normally, i.e., under no-fault conditions. To calculate the probability, a set of events are defined. The event $A_k$ represents that $\hat{a}_{1,k}$ is outside the two-sigma range at time $k$ under normal conditions. The false alarm rate therefore is expressed as $P(A_{k-n+1}, A_{k-n+2}, \ldots, A_k)$.

If traditional SPC without Kalman filtering is to be used, then, $\hat{a}_{1,j}, j = k-n+1, \ldots, k$, would be considered independent. The false alarm rate $P(A_{k-n+1}, A_{k-n+2}, \ldots, A_k)$ would thus equal $P(A_{k-n+1}) \cdot P(A_{k-n+2}) \cdot \ldots \cdot P(A_k)$, and could be easily calculated given the distributions of the estimates [3]. However, when the SPC is combined with Kalman filtering, $\hat{a}_{1,j}$, $j = k-n+1, \ldots, k$, are no longer independent because the estimate at time $j$, $\hat{a}_{1,j}$, is affected by the previous estimate $\hat{a}_{1,j-1}$ in the Markov process (13). Because of the Markov process, the false alarm rate should equal

$$P(A_{k-n+1}, \ldots, A_k) = P(A_{k-n+1}) \prod_{j=k-n+2}^{k} P(A_j | A_{j-1}). \tag{16}$$

To calculate $P(A_j|A_{j-1})$, our idea is to look into the Kalman filter equations to find out how the estimate at time $j$, $\hat{a}_{1,j}$, depends on the estimate at time $j-1$, $\hat{a}_{1,j-1}$. To do this, the re-

lationship between $\hat{x}_{j-1}$ and $\hat{x}_j$ is first obtained by substituting Kalman filter (9) to (13) as

$$\hat{x}_j = (1 - K_j H)\hat{x}_{j-1} + K_j H x_j + K_j v_j. \quad (17)$$

By assuming for simplicity that $K_j H$ in (17) is a diagonal matrix with elements $m_{1,j}$, $m_{2,j}$, and $m_{3,j}$, the relationship between $\hat{a}_{1,j}$ and $\hat{a}_{1,j-1}$ can be then obtained from (17) as

$$\hat{a}_{1,j} = (1 - m_{1,j})\hat{a}_{1,j-1} + m_{1,j} a_{1,j} + (K_j v_j)_1 \quad (18)$$

where $(K_j v_j)_1$ is the first element of the vector $K_j v_j$, $a_{1,j}$ is the true value of the parameter $a_1$ at time $j$, and $m_1 \in [0, 1]$. In the numerical testing, the values of $m_1$, $m_2$, and $m_3$ for the chiller are between 0.3 and 0.7 for most of the time. In (18), the first term on the right-hand side represents how the current estimation $\hat{a}_{1,j}$ is affected by the previous estimate $\hat{a}_{1,j-1}$. The last two terms on the right-hand side represent how $\hat{a}_{1,j}$ is affect by the current measurement.

Since the process noise and measurement noises are normal, the estimate $\hat{a}_{1,j}$ in (18) should be normally distributed. Based on (18) and the above assumption, the false alarm rate of the SPC rule with $n$ back-to-back estimates lying outside two-sigma range is calculated in detail in the Appendix. Using the (34) and (35) in the Appendix and assuming $m_1$ in (18) equal to 0.5, the false alarm rates with $n$ equal to 1, 2, and 3 are 6.71%, 1.50%, and 0.34%, respectively. Since three is the minimal value of n that has a false alarm rate less than 1%, $n$ is set to three in our SPC rule.

*Determining K to Obtain the Adaptive SPC Control Limits:* In the SPC rule, the means of parameters estimated over the past $K$ hours are used as the baseline of the normal range of a device parameter. If $K$ is too large, then adaptive means will be similar to static ones obtained from good data as in Fig. 4 and there will be many false alarms; if it is too small, then the means will shift gradually in the direction of the parameter estimated under faults and cannot be used as baselines to detect faults. For the detection of sudden faults, $K$ is set to 24 because: 1) no matter what design a building has, cooling load and model parameters have a pattern of 24 h due to both weather and hour schedules and 2) considering that the SPC rule requires estimates lying outside two-sigma range in several (e.g., three) consecutive hours, 24 h is long enough to detect a sudden fault as presented later in this section and also Section VI.

*Detecting Sudden Faults:* For illustration, a chiller in the HVAC system of the Shanghai Jinmao Tower is selected as an example (details of the HVAC system is in Section VI). A sudden drop of chiller capacity by 40% occurs to the chiller at the 5449th hour of a year (Aug. 16th). Estimated $a_1$ of the chiller gray-box model is shown in Fig. 6, together with the associated mean, one-sigma range and tow-sigma range. It can be seen that the estimated values fell outside the two-sigma range for more than three back-to-back hours at 5456th hour. Therefore, the fault was detected by $a_1$ 7 h after it happened. In addition, no false alarms are detected before the 5449th hour. More results about $a_2$ and $a_3$ and more insights are presented in the case study in Section VI.

When a fault is detected, calculating the process noise covariance matrix $Q$ based on the estimated process noises (10) will result large inaccuracy in $Q$. This is because the process noises estimated by (10) will include the parameters' deviation caused by the fault. Our idea is to remain $Q$ at its latest available value until parameters fall back to their two-sigma ranges and $m$ estimated process noises (10) become available again.

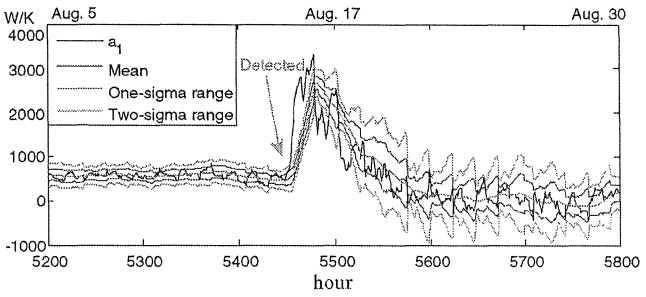


Fig. 5. The sudden drop of chiller capacity at the 5449th hour was detected by $a_1$ after $a_1$ fell outside the two sigma range over three back-to-back hours.

As shown in Fig. 5 after the detection of a fault, the mean of the parameter adjusted to the deviating parameter and fell back to its two-sigma range again. If the time interval between two successive sudden faults is large enough for the mean of a parameter to fall back, then the two faults can be detected separately.

*Reasons for Selecting Two-Sigma Range in the SPC Rule:* In our SPC rule, two-sigma range is chosen as SPC control limits. To maintain the false alarm rate below 1%, a fault is detected only after estimated parameters fall outside two-sigma range in three successive hours. Therefore, a fault might be detected at least three hours after it occurs. If one-sigma instead of two-sigma range is chosen in the SPC rule and the false alarm rate is still required to be below 1%, then six back-to-back estimates are required to lie outside one-sigma range to detect a fault. The detection time for one-sigma range might be 3 h later than that for two-sigma range. Therefore, two-sigma rather than one-sigma range is selected in our SPC rule.

If three-sigma range is used, the false alarm rate with one estimate lying outside three-sigma range is less than 1% since a normally distributed parameter under no-fault conditions has a probability of 99.7% to fall inside its three-sigma range. Although the detection time for three-sigma range might be two hours earlier than that for two-sigma range, the SPC rule with three-sigma range cannot detect small faults which cause a parameter falling outside the two-sigma range but still inside the three-sigma range.

### D. SPC Rule for Detecting Gradual Faults

If the SPC rule developed in the last subsection for sudden faults is directly adopted for gradual faults, these faults may not be detected. Consider a chiller in the HVAC system of the Shanghai Jinmao Tower for example. Gradual capacity degradation by 40% over a month occurs to the chiller from the 5449th hour of a year. The fault causes a device parameter, e.g., $a_1$, to shift gradually, as shown in Fig. 6. This gradual fault, however, is not detected by the SPC rule for sudden faults. This is because the gradual fault is too small to be detected within 24 h. After 24 h, even though the gradual fault becomes large, the means of $a_1$ over the last 24 h shift gradually in the direction of $a_1$. The fault

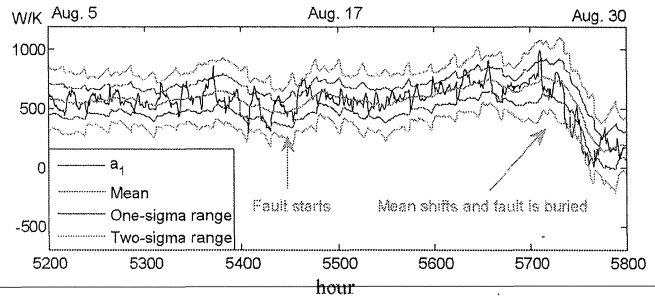


Fig. 6. Gradual degradation of chiller capacity by 40% over a month (from the 5449th hour to the 6169th hour) was not detected by $a_1$.

is therefore buried within this adaptive adjustment process, as shown in Fig. 6.

To detect gradual faults, our idea is still to use $n$ back-to-back estimates lying outside two-sigma range as the SPC rule, with the means of device parameters averaged over the past $K$ hours. No matter for detecting sudden or gradual faults, $n$ should be as low as possible but maintaining a false alarm rate below 1% as presented in the last subsection. Since the false alarm rate is calculated with devices working under normal conditions, it is not affected by the value of $K$. Therefore, the value of $n$ for sudden faults, i.e., three, is applied for gradual faults. As for $K$, its value for sudden faults (i.e., 24) cannot be adopted for gradual faults and an appropriate $K$ should be selected.

As presented in Section IV-C, to keep a balance between false alarm rate and detection rate, $K$ should be not too large or too small. For gradual faults, our idea is to set $K$ to a value as low as possible to reduce false alarm rate while maintaining a certain probability of detection (detection confidence), e.g., 99%, when a gradual fault becomes large to be detected. Therefore, we need to find the minimal value of $K$ that has a detection rate higher than 99%.

Consider a gradual fault that started at time $t_0$ and causes a parameter, e.g., $a_1$ to increase at a fixed rate of $s\sigma_1$ ($\sigma_1$ is the standard deviation of $a_1$ and $s$ is a given constant reflecting the severity of the fault) per hour over $\Delta T$ hours. After time $t_0+\Delta T$, $a_1$ becomes $a_1+s\sigma_1\Delta T$ (the affection of time-varying cooling load on the parameter is not considered to make it easy to roughly determine $K$). The probability of detecting a fault is not only affected by $K$ but also by the parameter's deviation rate $s\sigma_1$ and duration $\Delta T$. Although $s\sigma_1$ and $\Delta T$ in HVACs are usually not known in advance, their values of typical faults [28] can be used to study how the probability of detection is affected by $K$. This study can then provide a guide to roughly determine the value of $K$.

*Determining K Based on the Probability of Detection:* Consider $a_1$ of a chiller model as an example. To calculate the probability of detection under the above-mentioned gradual fault, a set of events are defined with event $B_t$ representing the estimated $\hat{a}_{1,t}$ being outside the two-sigma range at time $t$. Assume that the fault becomes large to be detected at time $t$ but not before that. Then, the probability of detection at time $t$ equals $P(B_{t-2}, B_{t-1}, B_t)$ as derived below.

Since $\hat{a}_1$ is governed by the Markov process (13), we have

$$P(B_{t-2}, B_{t-1}, B_t) = P(B_{t-2})P(B_{t-1}|B_{t-2})P(B_t|B_{t-1}). \tag{19}$$

The estimated $\hat{a}_{1,t}$ should be normally distributed since the process and measurement noises are normal. With the above assumption, the calculation of $P(B_t|B_{t-1})$ under the fault condition is very similar to that of $P(A_j|A_{j-1})$ (see (34) in the Appendix) under normal condition except that the mean of $\hat{a}_{1,t}$, $\hat{\mu}_{1,t}$, under the fault condition deviates from its normal value by $(t-t_0)s\sigma_1$ at time $t$. The probability of $P(A_j|A_{j-1})$ is therefore given by

$$\begin{aligned} P(B_t|B_{t-1}) = 1 - \int_{\hat{\mu}_{1,t-1}-[2-(t-1-t_0)s]\hat{\sigma}_{t-1}-\delta_{1,t-1}}^{\hat{\mu}_{1,t-1}+[2-(t-1-t_0)s]\hat{\sigma}_{t-1}-\delta_{1,t-1}} \\ \left(1 - \int_{\hat{\mu}_{1,t}-[2-(t-t_0)s]\hat{\sigma}_t-\delta_{1,t}}^{\hat{\mu}_{1,t}+[2-(t-t_0)s]\hat{\sigma}_t-\delta_{1,t}} \right. \\ \left. \times f(\hat{\mu}_{1,t}, \hat{\sigma}_{1,t}) d\hat{a}_{1,t} \right) f(\hat{\mu}_{1,t-1}, \hat{\sigma}_{1,t-1}) d\hat{a}_{1,t-1}. \end{aligned} \tag{20}$$

In the above, similar to (33), $\delta_{1,t}$ is a variable defined below to simplify the expression of (20), i.e.,

$$\delta_{1,t} = (1-m_{1,t})(\hat{a}_{1,t-1} - \overline{\mu}_{1,k}). \tag{21}$$

To complete the calculation of (19), $P(B_{t-1}|B_{t-2})$ is calculated similarly as $P(B_t|B_{t-1})$ in (20), and $P(B_{t-2})$ similarly to $P(A_{k-n+1})$ in (35) in the Appendix.

To maintain the probability of detection $P(B_{t-2}, B_{t-1}, B_t)$ above 99% at time $t$, we need to find the minimal value of $K$, $K_0$, as

$$K_0 = \arg\min_K P(B_{t-2}, B_{t-1}, B_t) > 99\%. \tag{22}$$

As $K$ increases, the mean of $\hat{a}_1$ over the last $K$ hours will be less affected by the fault and deviate more from the estimate $\hat{a}_{1,t}$. Therefore, the probability of detection at time $t$, $P(B_{t-2}, B_{t-1}, B_t)$, increases monotonically with $K$. The value of $K_0$ can then be easily obtained given the parameter's deviation rate $s\sigma_1$ and the duration $\Delta T$. For a gradual fault with $s\sigma_1 = 4\sigma_1$ and $\Delta T = 720$ h (i.e., the fault lasts gradually for a month), if $K$ is set to 720, then the probability of detection after 30 days is higher than 99%.

*Detecting Gradual Faults:* By calculating the means over the last 30 days (i.e., 720 h) and using three back-to-back points outside two-sigma range as the SPC rule, the 40% gradual degradation of chiller capacity over a month (i.e., the fault in Fig. 6) was detected after 12 days and 4 h, as shown in Fig. 7.

If the time interval between two gradual faults is large enough for device parameters to fall back into their two-sigma ranges, then the two faults can be detected separately. With $K$ equal to 720 (corresponding to 30 days), the means of parameters, however, adjust to the first fault so slowly that the time interval

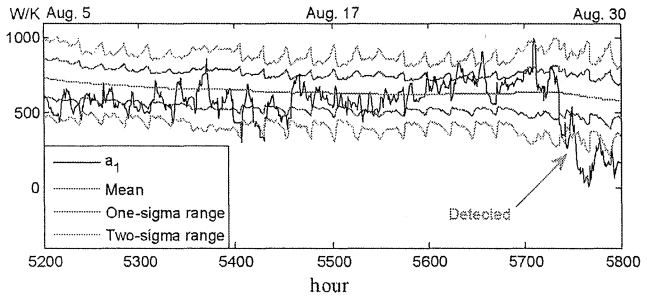


Fig. 7. The gradual chiller degradation was detected by $a_1$.

required for parameters falling back is usually too large to detect the second fault separately. Our idea to solve the problem is to adaptively adjust $K$. Once a fault is detected, $K$ is set to 24 and increases gradually to 720 as time goes so that the means of parameters can adjust to the deviating parameters as soon as possible. In this way, parameters can fall back to their two sigma-ranges fast to get ready for detecting the second fault separately.

### *E. Discussions*

Our method presented in this section is simply to perform SPC and Kalman filtering on individual devices and does not need to consider the interactions between different devices. In addition, gray-box models use physical knowledge together with measured data, and are more robust than black box models to different kinds of devices; and Kalman filtering is a well proven technology and does not need long-time focused studies when applied in individual devices in different buildings. The method can therefore detect both sudden faults and gradual degradation, both device faults and sensor faults (to be presented in next section) and can be easily replicated to HVAC systems with various devices.

As discussed in Section IV-C when a fault is detected, the process noise covariance matrix $Q$ should remain at its latest available value until parameters fall back to their two-sigma ranges. Since the time it takes for parameters to fall back is affected by the value of $K$, the values of $Q$ for the two SPC rules are different. Therefore, two Kalman filters are needed with one for detecting sudden faults and the other for gradual faults. One straightforward way to apply these two sets of Kalman filers and SPC rules in practice is to run them side by side.

There is a limitation of our method. If a gradual fault occurs at a rate slower than the parameters' normal drifting caused by time-varying cooling load, etc., the fault would be buried in the parameters' normal drifting and not be detected.

## V. Effects of Faults in One HVAC Subsystem on Another

A fault in one HVAC subsystem may affect another subsystem in terms of water or air temperature, energy consumption, etc., through the coupling of water or air flows between them. Consider for example a simple system with a chiller and a cooling tower. When the chiller capacity is reduced because of fouling in its evaporator, the chiller electric power $P_{ch}$ will increase to satisfy the cooling load $L_{ch}$. Then, electricity consumed by the chiller will be converted to heat and the heat will then become part of cooling load $L_c$ for the cooling tower. Therefore, symptoms such as the increased cooling water temperature $t_{ci}$ will show up even though nothing is wrong with the cooling tower.

As presented above, effects of the chiller fault can be detected in the cooling tower. A systematic analysis of the propagation of fault effects can help detect or confirm a device fault. In view that the gray-box models presented above describe device characteristics rather than flow balance or energy conservation, such system-wide analysis is not straightforward. Our idea is to introduce "coupling variables" between subsystems to capture their interactions. Consider the example of the previous paragraph. The cooling tower load $L_c$ is such a coupling variable since it can be predicted from the chiller gray-box model, and can also be easily calculated from measured variables of the cooling tower as presented below.

To calculate $L_c$ from cooling tower measured variables, it is expressed as the energy difference between inlet and outlet cooling water in the cooling tower, i.e.,

$$L_c = C_w g_{wc}(t_{ci} - t_{co}) \tag{23}$$

where $g_{wc}$ is the cooling water flow rate, and $t_{ci}$ and $t_{co}$ are inlet and outlet cooling water temperatures, respectively, as in Fig. 2.

To predict $L_c$ from the chiller gray-box model, it is necessary to derive the relationship between $L_c$ and chiller model parameters. From the perspective of the chiller, electricity consumed by the chiller will be converted to heat and then become part of cooling tower load $L_c$. Therefore, $L_c$ equals the sum of chiller electric power $P_{ch}$ and chiller cooling load $L_{ch}$, i.e.,

$$L_c = P_{ch} + L_{ch}. \tag{24}$$

In (24), $L_{ch}$ can be calculated from measured variables by (2) and from the definition of COP (defined as the ratio of chiller cooling load $L_{ch}$ to chiller power $P_{ch}$), $P_{ch}$ can be predicted as

$$P_{ch} = \frac{L_{ch}}{\mathrm{COP}}. \tag{25}$$

In (25), COP can be predicted from chiller model parameters of the gray box model (1). To predict COP under normal, i.e., no-fault conditions, the normal values of model parameters are required. They, however, are difficult to obtain since they are affected by the cooling load and are time varying. In our method, the average value of a parameter over the past some, e.g., 30, days as predicted by the Kalman filter is used as its approximate normal value. After predicting the normal value of COP based on the means of parameters, $L_c$ can then be predicted from (24) and (25).

Generally, the selection of coupling variables should follow two guidelines: 1) they are measurable or easily calculated from measured variables in the subsystem which is affected by a fault and 2) they are an explicit function of gray-box model parameters of the coupling subsystem so that their values under normal, i.e., no-fault conditions, can be predicted based on these parameters. When a fault in one subsystem affects another, then the coupling variable's predicted value under normal conditions

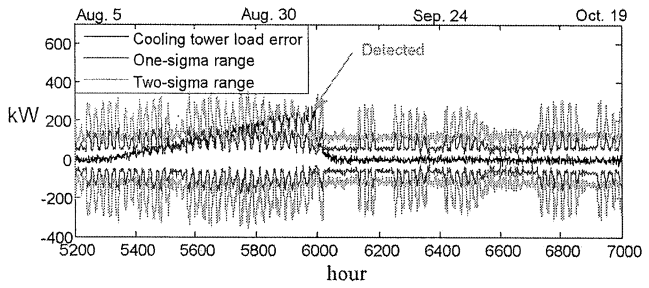


Fig. 8. Gradual chiller capacity degradation was detected by the error terms between measured and predicted cooling tower load.

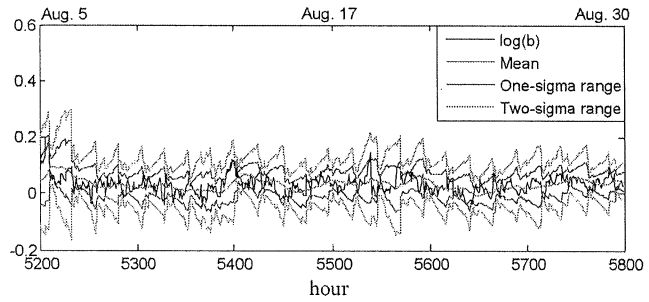


Fig. 9. No fault was detected by $log\ b$ in the cooling tower model with gradual chiller capacity degradation.

will deviate from its value measured under faulty conditions. The SPC rule can then be used to detect the fault based on the error term between the measured and predicted values.

For the above example, after obtaining the predicted and measured values of $L_c$, the errors between them can be calculated. The SPC rule which uses three back-to-back points outside two-sigma range to detect faults is then performed on the error term of $L_c$. The normal values of the error term should be zero, so the SPC control limits are the two-sigma range of the error term around zero means. Since the errors term is derived based on the chiller gray-box model parameters, the standard deviations of the error terms are derived from standard deviations of chiller parameters using Monte Carlo simulation. As shown in Fig. 8, the chiller fault is detected by the error term of coupling variable $L_c$. In addition, no fault is detected by $log\ b$ (or $m$ or $n$) of the cooling tower model, as shown in Fig. 9. We shall then be able to tell that: 1) there is no fault in the cooling tower and 2) the chiller fault detected by the chiller gray-box model in Section IV-D is confirmed.

The above method of analyzing the propagation of fault effects from one subsystem on another is simply performing SPC on coupling variables. There is no need to create a big Kalman filter for the aggregate model of coupled subsystems. Therefore, there is no major increase in complexity as compared to the device-level fault detection except the addition of coupling variables and the associated SPC rules. Our method thus has good scalability and can be easily replicated to large buildings.

## VI. A Case Study for Shanghai Jinmao Tower

Our method developed above is tested against the Jinmao Tower, a famous building in Shanghai. Its HVAC system is introduced in Section VI-A. It is of large scale and with a complex configuration. This system has been used earlier in Section IV to help illustrate our method. It is now used to demonstrate that the method can handle complications specific to a high-rise building in terms of complicated analysis. Five fault cases are considered: sudden chiller capacity degradation in Section VI-B, gradual chiller capacity degradation in Section VI-C, gradual chiller sensor deviation in Section VI-D, sudden fault of the cooling tower fan in Section VI-E, and effects of chiller faults on cooling towers in Section VI-F. The fault detection in the first two cases involves only a single chiller and is easy to be duplicated with required data provided for that chiller. Their data sets and testing results are available at https://docs.google.com/#folders/0B-5BNyF3W-H7dDNN-ODFmb0hSbGk0OHZQbmJkZ2hUUQ.

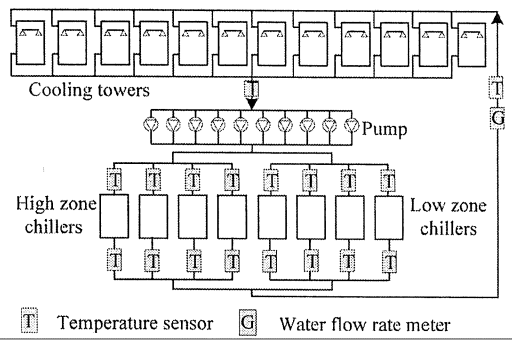


Fig. 10. Cooling water flow in the Jinmao Tower with 12 cooling towers and eight chillers.

### A. Jinmao Tower and Its HVAC System

The Jinmao Tower is a 420-meter-high famous building in Shanghai. It has 88 floors, with the third to the 50th floor used as offices and the 58th to the 85th floor as a hotel. Its main HVAC system is composed of 12 cooling towers and eight chillers in a typical structure, as shown in Fig. 10. All the cooling towers are for the entire building, while four of the chillers are for the high zone (floors above and including the 23rd floor) and the other four for the low zone. We are concerned with the fault detection in the 12 cooling towers, the four chillers for the high zone, and the air handling units (AHUs, each for one floor) in high zone office floors.

For the cooling water flowing between cooling towers and chillers as shown in Fig. 10, it is first mixed after coming out of cooling towers and then supplied to eight chillers via a single main pipe. After coming out of chillers, cooling water is mixed and then returns to cooling towers. As for the chilled water flowing between four chillers and AHUs in high zone, as shown in Fig. 11, chilled water from the four chillers first flows into a water segregator and is then distributed to different AHUs. Also, chilled water returning from AHUs is first collected in a water collector and then flows back to the four chillers.

The simulation model used to simulate the operation of the HVAC system was developed in the software "Designer's Simulation Toolkit (DeST)" [26], [27]. It was developed by the Department of Building Science, Tsinghua University and has been widely used in China. Its results have been validated by selected

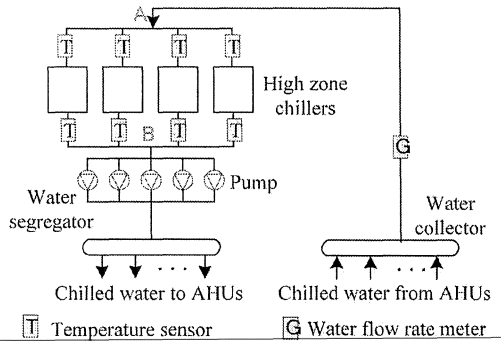


Fig. 11. Chilled water flow with four chillers for the high zone.

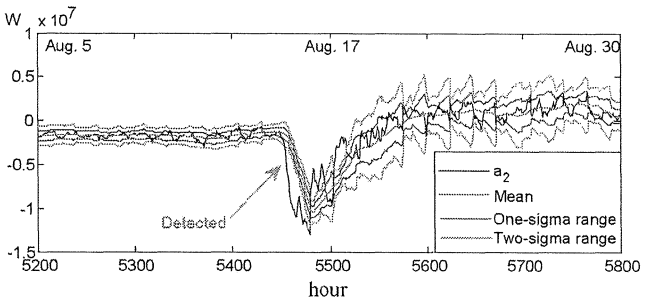


Fig. 12. The sudden fault of chiller capacity degradation was detected by $a_2$.

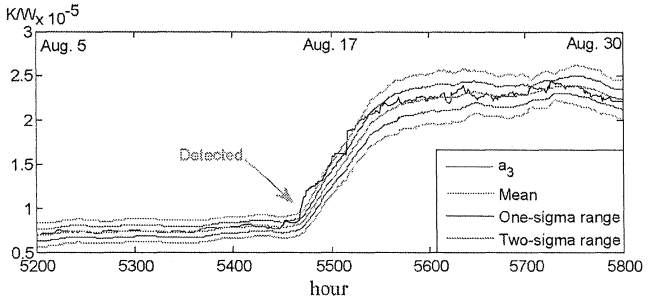


Fig. 13. The sudden fault of chiller capacity degradation was detected by $a_3$.

buildings and comparison with simulation results of other software, including Energy Plus. To obtain the cooling load for the HVAC system in the year of 2006 [29], we did not simulate the entire building but only simulate the office floors and use measured cooling load in the hotel floors, because data required by the simulation for the hotel floors, such as number of occupants, was not available to us. Although in simulation we have access to all the information, for fault detection we only use measured variables that correspond to real sensors outputs in the Jinmao Tower.

Since the Jinmao Tower has many sensors, most variables required by Kalman filters are available in the Jinmao Tower. Other variables required nevertheless can be derived. Consider fault detection for a chiller for example. In the chiller gray box model (1), all the measured variables can be directly measured in the Jinmao Tower, except the chilled water flow rate $g_{wch}$. It nevertheless can be derived from the mixed chilled water flow rate (measured in the Jinmao Tower) based on water pressure balance and water flow balance as presented below.

From water pressure balance in the high-zone chiller subsystem in Fig. 11, water pressure drops from Point A to Point B in all branches containing a chiller that is on (there is no water flow in a chiller if it is off) should be the same, i.e.,

$$\Delta p_{ABi} = \Delta p_{ABj}, \quad i \neq j \in J \tag{26}$$

where $\Delta p_{ABj}$ is water pressure drop for branch $j$, and $J$ is the set of chillers that are on. The pressure drop $\Delta p_{ABj}$ is a quadratic function of that branch's water flow rate $g_{wchj}$, i.e., [23]

$$\Delta p_{ABj} = S_j g_{wchj}^2, \quad j \in J \tag{27}$$

where $S_j$ is the drag coefficient of branch $j$ from manufacture specifications.

From water flow balance, the sum of chilled water flow rates in all chillers should equal the measured mixed chilled water flow rate $g_{wch,mix}$, i.e.,

$$\sum_{j=1}^{J} g_{wchj} = g_{wch,mix}. \tag{28}$$

From (26)–(28), chilled water flow rates $g_{wchj}$ for individual chillers can be calculated. Then all the variables needed in the chiller gray-box model are available for chiller fault detection. For cooling tower fault detection, cooling water flow rates can be similarly calculated. With the above calculation, our method can be easily implemented in the HVAC system of large-scale buildings.

For the three cases in the following subsections, our fault detection method did not know in advance how many faults there were, what kinds of faults they were, or when they started. The only thing the method knew was that faults were generated after the 5200th hour (August 5) of that year. In addition, the first time the method is applied in the Jinmao Tower, devices are required to work without any faults for a certain period of time so as to ensure device gray-box model parameters can converge to their normal values. In the simulation, our fault detection method was applied from the 5000th hour, and the time period of eight days from the 5000th hour to the 5199th hour was enough for parameters to converge.

Since the three cases consider chiller faults and their effects on the 12 cooling towers, the SPC is performed on model parameters of the chiller with faults and the 12 individual cooling towers, and then the coupling variable between chiller and cooling tower subsystems.

### *B. Sudden Chiller Capacity Degradation*

A sudden chiller capacity degradation by 40% was considered. The degradation was generated in the DeST model by reducing the COP by 40%. The fault started from August 16 (the 5449th hour of the year) and lasted to the end of the year. By using our method for detecting sudden faults, the three chiller gray-box model parameters together with their means, one-sigma ranges, and two-sigma ranges are shown in Figs. 5, 12, and 13, respectively. It can be seen that the fault was detected by all the three parameters within 24 hours after it occurred.

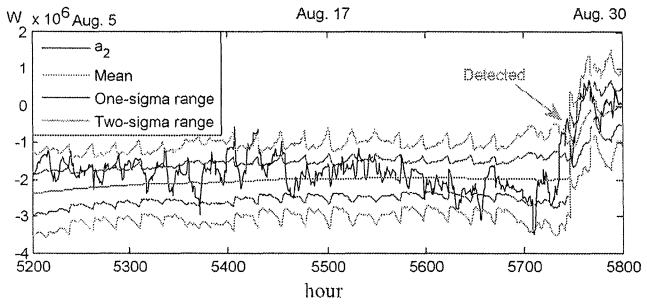


Fig. 14. The gradual fault was detected by $a_2$ after 10 days and 21 h.

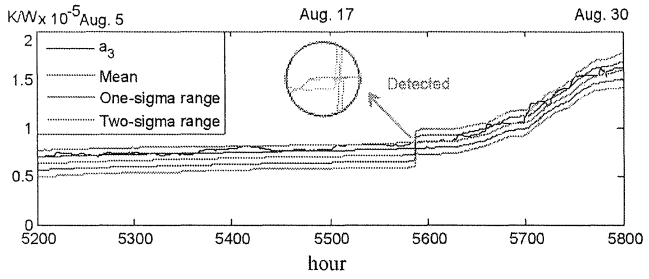


Fig. 15. The gradual fault was detected by $a_3$ after 6 days and 19 h.

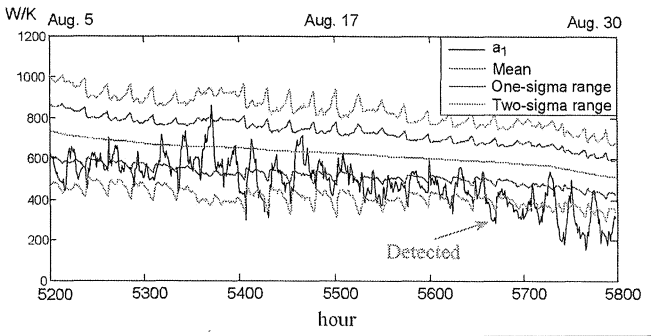


Fig. 16. The gradual sensor fault for $t_{ci}$ was detected by $a_1$ after 9 days and 6 h.

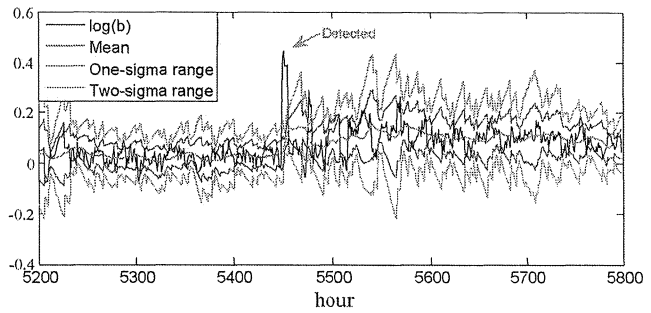


Fig. 17. The fault in the cooling tower fan was detected by the parameter $b$ after 4 h.

It should be noted that each of the three parameters has a specific physical meanings, e.g., $a_3$ is related to the evaporator and the condenser. The fault was detected by all the three parameters rather than one specific parameter related to a chiller component where the fault lies. That is because the chiller model within DeST is also a gray-box model, although more detailed than [1]. The only way to generate the fault was to reduce the COP. The COP, however, is related to all the three parameters. If the fault is generated based on a physical chiller model, these physical meanings of model parameters can be used for diagnosis. For example, if a fault is detected only by $a_3$, it can be isolated in the evaporator or condenser.

Since fault detection in this case only focuses on the faulty chiller, the duplication of the fault detection is easy with all variables required by Kalman filter provided, including the chilled water flow rate $g_{wch}$ calculated from (25)–(28) and water temperatures $t_{ci}$, $t_{chr}$, and $t_{chs}$ in the chiller gray box model. Complete data sets and testing results are provided for duplication on the website. In addition, from the testing results, it can be easily validated that the $K_jH$ matric is diagonally dominant, i.e., the diagonal element is greater than both the sum of all absolute values of other elements in the same row and that in the same column. Therefore, it is reasonable to assume $K_jH$ to be a diagonal matrix before (18).

### C. Gradual Chiller Capacity Degradation

The gradual chiller capacity degradation was generated by reducing the COP gradually by 40% over a month, i.e., 1.33% per day, from August 16 (the 5449th hour) to September 15 (the 6169th hour). After September 15, the chiller performed at 40% of its capacity. As shown in Figs. 7, 14, and 15, by using our method for gradual faults, the fault was detected by $a_1$, $a_2$ , and $a_3$ in 12 days, 11 days, and 7 days, respectively, after it happened. The fault was first detected by $a_3$ when the chiller capacity degraded only by 9%. The duplication of this case is also easy with values of the same data set as in Section VI-B provided on the website.

### D. Gradual Fault in a Chiller Sensor

To demonstrate the generality of our fault detection method, a fault in the sensor for measuring the mixed inlet cooling water temperature to chillers $t_{ci}$ is considered. The measured temperature deviates gradually above its true value for 1° over a month, i.e., 0.03° per day, August 16 (the 5449th hour) to September 15 (the 6169th hour). Since fans in cooling towers are controlled to satisfy the set point for $t_{ci}$ based on that sensor, true value of the $t_{ci}$ will deviate gradually below its set point. As shown in Fig. 16, it can be seen that the fault was detected by $a_1$ in 10 days.

### E. Sudden Fault in the Fan of a Cooling Tower

If there is a fault in the fan, the air flow rate obtained from the lookup table based on the fan frequency would deviate from the actual air flow rate. Using the improper airflow as an input to the cooling tower model would cause estimated parameters deviating from their normal ranges and cause the fault detected. A fault in a cooling tower fan was generated in the DeST model by reducing the air flow rate by 10%. The fault started from August 16 (the 5449th hour of the year) and lasted to the end of the year. By using our method for detecting sudden faults, the fault was detected four hours after it occurred, as shown in Fig. 17.

In the above four subsections, our fault detection method detect both sudden faults and gradual degradation, both device

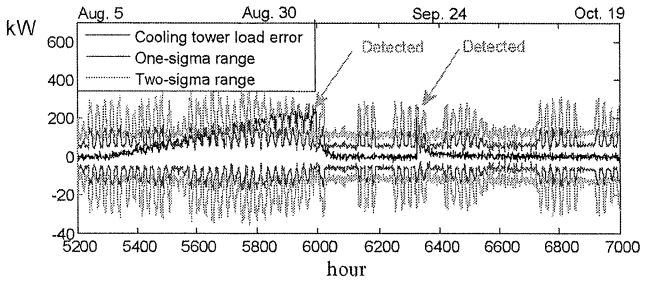


Fig. 18. Two chiller faults were detected by cooling tower load error term.

faults and sensor faults with no false alarms in the large-scale building, Shanghai Jinmao Tower. The method therefore should be robust to various faults.

### *F. Effects of Chiller Faults on Cooling Towers*

Sudden and gradual chiller capacity degradations in Sections VI-B and VI-C are used as an example to study the effects of faults in one subsystem on another. Two faults happened in sequence in a chiller. The first one was a gradual fault starting from the 5350th hour of the year. The second one was a sudden fault starting from the 6320th hour. The two faults were generated in the same way as in the last two subsections. The cooling tower cooling load $L_c$ was used as a coupling variable to detect the effects of the chiller faults on the cooling tower subsystem. The faults were fixed after they were detected by $L_c$.

As presented in Fig. 18, by performing our SPC rule on the errors between measured and predicted values of $L_c$, the effects of two chiller faults on cooling towers were detected in 25 days and in 14 h, respectively, after they happed. Meanwhile, no fault was detected in the cooling tower subsystem. Therefore, it can be concluded that nothing was wrong with the cooling tower subsystem and there were two faults in the chiller.

The two chiller faults were also be detected by the parameters of that chiller in seven days and in 6 h, respectively. The detection time of the chiller faults' effects on cooling towers, however, was later than that of the chiller faults. That was because of the low sensitivity of the coupling variable $L_c$ to chiller faults, since $L_c$ was affected by all the eight chillers while only one of them had faults. Therefore, the detection of the effects of chiller faults on cooling towers was also a confirmation of the detected chiller faults if the chiller is not fixed timely.

## VII. Conclusion

Fault detection of HVAC systems is difficult in view that the HVAC systems are large in scale, consisting of many coupling subsystems, building and equipment dependent, and working under time-varying conditions. In this paper, a data-driven method based on gray-box models with insights and understanding for system-level fault detection is developed. The method is a novel and synergistic integration of proven techniques of: 1) SPC for measuring and analyzing variations; 2) Kalman filtering based on gray-box models to provide predictions and to determine SPC control limits; and (3) system analysis for analyzing propagation of faults' effects across subsystems. The method has been tested against a simulation model of the HVAC system in the Shanghai Jinmao Tower with good results.

Our method can be easily replicated to HVAC systems with various devices because: 1) gray-box models use physical knowledge together with measured data, and are more robust than black box models to different kinds of devices; 2) Kalman filtering is a well proven technology and does not need long-time focused studies when applied in individual devices in different buildings; and 3) our method is simply device-level fault detection plus SPC on coupling variables, and does not need to create a big Kalman filter for coupling subsystems when used to detect propagation of faults' effects across subsystems.

The contribution of our work is that we developed a fault detection method which can detect both device faults and propagation of faults' effects across subsystems. The method has good replicability and scalability. Furthermore, it is simple and generic, and should be of significant interest to many other systems, like manufacturing systems.

## Appendix
## Calculation of the False Alarm Rate

This Appendix is to derive the probabilities of $P(A_j|A_{j-1})$ and $P(A_{k-n+1})$ which are used in (16) to calculate the false alarm rate of the SPC rule for sudden faults.

The probability $P(A_j|A_{j-1})$ represents the probability of the estimate $\hat{a}_{1,j}$ at time $j$ lying outside its two-sigma range $[\overline{\mu}_{1,j} - 2\overline{\sigma}_{1,j}, \overline{\mu}_{1,j} + 2\overline{\sigma}_{1,j}]$ conditioned on that the estimate $\hat{a}_{1,j-1}$ at time $j-1$ is already outside the two-sigma range. It is given by

$$P(A_j|A_{j-1}) = P\left(\hat{a}_{1,j} \notin [\overline{\mu}_{1,j} - 2\overline{\sigma}_{1,j}, \overline{\mu}_{1,j} + 2\overline{\sigma}_{1,j}] \middle| \hat{a}_{1,j-1} \notin [\overline{\mu}_{1,j-1} - 2\overline{\sigma}_{1,j-1}, \overline{\mu}_{1,j-1} + 2\overline{\sigma}_{1,j-1}]\right). \quad (29)$$

In the above, $\overline{\mu}_{1,j}$ is the mean of $\hat{a}_1$ over the past $K$ hours and is defined in (15), and $\overline{\sigma}_{1,j}$ is the averaged standard deviation of $\hat{a}_1$ over the past $K$ hours.

With all the estimates normally distributed, from (29), we have

$$P(A_j|A_{j-1}) = 1 - \int_{\overline{\mu}_{1,j-1}-2\overline{\sigma}_{1,j-1}}^{\overline{\mu}_{1,j-1}+2\overline{\sigma}_{1,j-1}} \left(1 - \int_{\overline{\mu}_{1,j}-2\overline{\sigma}_{1,j}}^{\overline{\mu}_{1,j}+2\overline{\sigma}_{1,j}} f(\hat{\mu}_{1,j}, \hat{\sigma}_{1,j}) d\hat{a}_{1,j}\right) \times f(\hat{\mu}_{1,j-1}, \hat{\sigma}_{1,j-1}) d\hat{a}_{1,j-1} \quad (30)$$

where $f(\hat{\mu}_{1,j}, \hat{\sigma}_{1,j})$ is the normal probability density function of $\hat{a}_{1,j}$ with mean $\hat{\mu}_{1,j}$ and standard deviation $\hat{\sigma}_{1,j}$.

To calculate $P(A_j|A_{j-1})$ in (30), the relationship between $\overline{\mu}_{1,j}$ and $\hat{\mu}_{1,j}$ and that between $\overline{\sigma}_{1,j}$ and $\hat{\sigma}_{1,j}$ are needed. The first relationship can be obtained from (18) by taking the mean of both sides and assuming the true value $a_{1,j}$ of the parameter approximately equal to $\overline{\mu}_{1,j}$

$$\mu_{1,j} = (1 - m_{1,j})\hat{a}_{1,j-1} + m_{1,j}\overline{\mu}_{1,j}. \quad (31)$$

From (30), the relationship between $\overline{\mu}_{1,j}$ and $\hat{\mu}_{1,j}$ can be expressed as

$$\overline{\mu}_{1,j} = \hat{\mu}_{1,j} - \delta_{1,j}, \quad (32)$$

$$P(A_j|A_{j-1}) = 1 - \int_{\hat{\mu}_{1,j-1}-2\sigma_{1,j-1}-\delta_{1,j-1}}^{\hat{\mu}_{1,j-1}+2\sigma_{1,j-1}-\delta_{1,j-1}} \left(1 - \int_{\hat{\mu}_{1,j}-2\sigma_{1,j}-\delta_{1,j}}^{\hat{\mu}_{1,j}+2\sigma_{1,j}-\delta_{1,j}} f(\hat{\mu}_{1,j}, \hat{\sigma}_{1,j}) d\hat{a}_{1,j}\right) f(\hat{\mu}_{1,j-1}, \hat{\sigma}_{1,j-1}) d\hat{a}_{1,j-1} \quad (34)$$

where $\delta_1$ is a variable defined below to simplify the expression of (32):

$$\delta_{1,j} = (1 - m_{1,j})(\hat{a}_{1,j-1} - \overline{\mu}_{1,j}). \quad (33)$$

For simplicity, the averaged standard deviation $\overline{\sigma}_{1,j}$ is assumed approximately equal to the standard deviation of $\hat{a}_{1,j}, \hat{\sigma}_{1,j}$, in the long run. Then, by substituting (32) and $\overline{\sigma}_{1,j} = \hat{\sigma}_{1,j}$ into (30), we have equation (34) shown at the top of the page.

Similarly, the probability $P(A_{k-n+1})$ in (16) is calculated as

$$P(A_{k-n+1}) = 1 - \int_{\hat{\mu}_{1,k-n+1}-2\hat{\sigma}_{1,k-n+1}-\delta_{1,k-n+1}}^{\hat{\mu}_{1,k-n+1}+2\hat{\sigma}_{1,k-n+1}-\delta_{1,k-n+1}} f(\hat{\mu}_{1,k-n+1}, \hat{\sigma}_{1,k-n+1}) \times d\hat{a}_{1,k-n+1}. \quad (35)$$

By substituting (34) and (35) into (16) and using the value of $m_{1,j}$ in the numerical testing, the false alarm rate $P(A_{k-n+1}, A_{k-n+2}, \ldots, A_k)$ of the SPC rule for sudden faults can be calculated.

## ACKNOWLEDGMENT

The authors would like to thank the United Technology Research Center (UTRC) and many individuals for their generous support. Special thanks to S. Narayanan, R. Munoz, M. Atalla, C. Walker, T. Bailey, I. Cohen, B. LaBarre, G. Poncia, R. Brahme, B. Hobbs, and D. Parekh of UTRC; M. McQuade and C. Pietrzykowski of UTC; Y. Jiang and P. Peng of UTRC China; and Z. Jiang, Department of Building Science, Tsinghua University and Y. Chen, Department of Electrical and Computer Engineering, University of Connecticut.

## REFERENCES

[1] B. Sun, P. B. Luh, Z. O'Neill, and F. Song, "Building energy doctors: SPC and Kalman filter-based fault detection," in *Proc. IEEE Conf. Autom.Sci. Eng.*, Trieste, Italy, Aug. 2011, pp. 333–340.

[2] J. Lausten, *Energy Efficiency Requirements in Building Codes, Energy Efficiency Policies for New Buildings*. Paris, France: International Energy Agency, 2008.

[3] B. Fournier, N. Rupin, M. Bigerelle, D. Najjar, and A. Iost, "Comments on the mixture detection rule used in SPC control charts," *Communications in Statistics—Simulation and Computation*, vol. 36, no. 6, pp. 1321–1331, 2007.

[4] B. Sun, P. Luh, and Z. O'Neill, "SPC and Kalman filter-based fault detection and diagnosis for an air-cooled chiller," *Frontiers of Electr. Electron. Eng.*, vol. 6, no. 3, pp. 412–423, 2011.

[5] I. B. D. McIntosh, J. W. Mitchell, and W. A. Beckman, "Fault detection and diagnosis in chillers, part 1: Model development and application," *ASHRAE Trans.*, vol. 106, no. 2, pp. 268–282, 2000.

[6] K. Choi, S. M. Namburu, M. S. Azam, J. Luo, K. R. Pattipati, and A. Patterson-Hine, "Fault diagnosis in HVAC chillers using data-driven techniques," in *Proc. IEEE Autotestcon*, 2004, pp. 407–413.

[7] M. S. Breuker and J. E. Braun, "Evaluating the performance of a fault detection and diagnostic system for vapor compression equipment," *Int. J. Heating, Ventilating, Air Conditioning and Refrigerating Res.*, vol. 4, no. 4, pp. 401–425, 1998.

[8] S. M. Namburu, M. S. Azam, J. Luo, K. Choi, and K. R. Pattipati, "Data-driven modeling, fault diagnosis and optimal sensor selection for HVAC chillers," *IEEE Trans. Autom. Sci. Eng.*, vol. 4, no. 3, pp. 469–473, Jul. 2007.

[9] S. W. Wang and F. Xiao, "AHU sensor fault diagnosis using principal component analysis method," *Energy and Buildings*, vol. 36, pp. 147–160, 2004.

[10] S. W. Wang and J. T. Cui, "Sensor-fault detection, diagnosis and estimation for centrifugal chiller systems using principal component analysis method," *Appl. Energy*, vol. 82, pp. 197–213, 2005.

[11] J. Y. Qin and S. W. Wang, "A fault detection and diagnosis strategy of VAV air-conditioning systems for improved energy and control performances," *Energy and Buildings*, vol. 37, pp. 1035–1048, 2005.

[12] O. Morisot and D. Marchio, "Fault detection and diagnosis on HVAC variable air volume system using artificial neural network," in *Proc. IBPSA Building Simulation*, Kyoto, Japan, 1999.

[13] T. M. Rossi and J. E. Braun, "A statistical, rule-based fault detection and diagnostic method for vapor compression air conditioners," *Int. J. Heating, Ventilating, Air Conditioning and Refrigerating Res.*, vol. 3, no. 1, pp. 19–37, 1997.

[14] A. Bashi, V. P. Jilkov, and X. R. Li, "Fault detection for systems with multiple unknown modes and similar units and its application to HVAC," *IEEE Trans. Control Syst. Technol.*, vol. 19, no. 5, pp. 957–968, Sep. 2011.

[15] J. Ru and X. R. Li, "Variable-structure multiple-model approach to fault detection, identification, and estimation," *IEEE Trans. Control Syst. Technol.*, vol. 16, no. 5, pp. 1029–1038, Sep. 2008.

[16] J. Saththasivam and K. C. Ng, "Predictive and diagnostic methods for centrifugal chillers," *ASHRAE Trans.*, vol. 114, no. 1, pp. 282–287, 2008.

[17] S. Katipamula and M. R. Brambley, "Methods for fault detection, diagnostics, and prognostics for building systems—A review, Part I," *Int. J. Heating, Ventilating, Air Conditioning and Refrigerating Res.*, vol. 11, no. 1, pp. 3–25, 2005.

[18] Y. E. Shao and J. Fu, "A fault detection for a correlated process with the use of SPC/EPC/NN scheme," in *Proc. 4th Int. Conf. Innovative Comput., Inform. Control (ICICIC)*, Kaohsiung, Taiwan, Dec. 7–9, 2009, pp. 240–243.

[19] N. M. Ung and L. Wee, "Fiducial registration error as a statistical process control metric in image-guidance radiotherapy with fiducial markers," *Phys. Med. Bio.*, vol. 56, pp. 7473–7485, 2011.

[20] J. M. Gordon and K. C. Ng, *Cool Thermodynamics*. Cambridge, U.K.: Cambridge Int. Sci., 2000.

[21] W. Jiang and T. A. Reddy, "Reevaluation of the Gordon-Ng performance models for water-cooled chillers," *ASHRAE Trans.*, vol. 109, no. 2, 2003.

[22] J. Lichtenstien, "Performance selection of mechanical draft cooling towers," *Trans. Amer. Soc. Mech. Eng.*, vol. 65, 1943.

[23] R. Y. Zhao, C. Y. Fan, and D. H. Xue, *Air Conditioning* (in Chinese). Beijing, China: China Construction Industry Press, 2009.

[24] Y. Bar-Shalom and X. R. Li, *Estimation and Tracking-Principles, Techniques, and Software*. London, U.K.: Artech House, 1993.

[25] G. Bishop and G. Welch, "An introduction to the Kalman filter," in *Proc. ACM SIGGRAPH, Course 8*, Los Angeles, CA, Aug. 2001.

[26] DeST software, Dept. Building Science, Tsinghua University, Beijing, China, 2008. [Online]. Available: www.dest.com.cn

[27] D. Yan, J. Xia, W. Tang, F. Song, X. Zhang, and Y. Jiang, "DeST—An integrated building simulation toolkit Part I: Fundamentals," *Building Simulation*, vol. 1, no. 5, pp. 95–110, 2008.

[28] M. S. Breuker and J. E. Braun, "Evaluating the performance of a fault detection and diagnostic system for vapor compression equipment," *Int. J. Heating, Ventilating, and Air Conditioning and Refrigerating Res.*, vol. 4, no. 4, pp. 401–425, 1998.

[29] P. Luh and B. Sun, Energy doctors: SPC and Kalman filter-based fault detection and diagnosis United Technology Research Center, Hartford, CT, UTRC Rep., 2010.

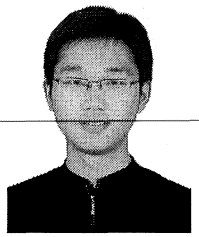

**Biao Sun** (S'11) received the B.E. degree in automation from Tsinghua University, Beijing, China, in 2006. He is currently working towards the Ph.D. degree at the Center for Intelligent and Networked Systems (CFINS), Department of Automation, TNLIST, Tsinghua University.

His research interests include optimal control for building energy savings, and fault detection and diagnosis of heating ventilation and air conditioning systems (HVAC).

**Peter B. Luh** (S'77–M'80–SM'91–F'95) received the B.S. from National Taiwan University, Taipei, the M.S. degree from the Massachusetts Institute of Technology (MIT), Cambridge, and the Ph.D. degree from Harvard University, Cambridge, MA.

He has been with the Department of Electrical and Computer Engineering, University of Connecticut since 1980, and currently is the SNET Professor of Communications and Information Technologies. He served as the Head of the Department from 2006 to 2009. He is also a member of the Chair Professors Group in the Department of Automation, Tsinghua University, Beijing, China. His interests include intelligent manufacturing systems—planning, scheduling, and coordination of design, manufacturing, and service activities; Smart, green and safe buildings—optimized energy management, HVAC fault detection and diagnosis, emergency crowd guidance, and eco communities; smart power systems—smart grid, design of auction methods for electricity markets, robust renewable (wind and solar) integration to the grid, electricity load and price forecasting with demand response, and micro grid; and mathematical optimization of large-scale mixed-integer problems, and decision-making under uncertain, distributed, or antagonistic environments.

Dr. Luh is the Senior Advisor on Automation for the Robotics and Automation Society. He was the VP of Publication Activities for the IEEE Robotics and Automation Society (2008–2011), the founding Editor-in-Chief of the IEEE TRANSACTIONS ON AUTOMATION SCIENCE AND ENGINEERING (2003–2007), and the Editor-in-Chief of the IEEE TRANSACTIONS ON ROBOTICS AND AUTOMATION (1999–2003).

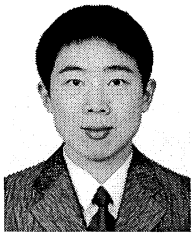

**Qing-Shan Jia** (S'02–M'06–SM'11) received the B.E. degree in automation in July 2002 and the Ph.D. degree in control science and engineering in July 2006, from Tsinghua University, Beijing, China.

He is an Associate Professor at the Center for Intelligent and Networked Systems (CFINS), Department of Automation, TNLIST, Tsinghua University, Beijing, China. He was a Visiting Scholar at Harvard University in 2006, and a Visiting Scholar at the Hong Kong University of Science and Technology in 2010. His research interests include theories and applications of discrete event dynamic systems (DEDSs) and simulation-based performance evaluation and optimization of complex systems.

**Zheng O'Neill** received the Ph.D. degree in mechanical engineering from the Building and Environmental Thermal Systems Research Group, Oklahoma State University, Stillwater, in 2004.

She is a Staff Research Engineer and Principal Investigator at the System Dynamics and Optimization Group in United Technologies Research Center where she has been since 2006. Her expertise is in building technology covering integrated building energy and control systems design, modeling and optimization, building commissioning, real-time decision support system in buildings for fault detection and diagnostics, and low energy/net zero energy buildings.

Dr. O'Neill is a registered Professional Engineer. She currently serves as a technical committee member for ASHRAE TC 7.5 Smart Building Systems. She is also a member of the Board of Directors of the International Building Performance Simulation Association (IBPSA) USA.

**Fangting Song** received the B.E. degree in heating ventilation and air conditioning systems (HVAC) in July 2001 from Chongqing University, Chongqing, China, and the Ph.D. degree in building and system simulation in January 2010 from Tsinghua University, Beijing, China.

She is a Senior Research Engineer at the United Technologies Research Center (UTRC, China). She is one of the key members of the Tsinghua-UTC Research Institute for Building Energy, Safety and Control Systems. Her research interests include building environment simulation, HVAC system simulation, integrated control of building systems, and new terminal control method.